United States Department of Commerce
Technology Administration
National Institute of Standards and Technology

NIST Technical Note 1398

Portable Calibrator for Across-the-Road Radar Systems

Arthur R. Ondrejka
Robert T. Johnk

NIST Technical Note 1398

Portable Calibrator for Across-the-Road Radar Systems

Arthur R. Ondrejka
Robert T. Johnk

Electromagnetic Fields Division
Electronics and Electrical Engineering Laboratory
National Institute of Standards and Technology
325 Broadway
Boulder, Colorado 80303-3328

May 1998

U.S. DEPARTMENT OF COMMERCE, William M. Daley, Secretary
TECHNOLOGY ADMINISTRATION, Gary R. Bachula, Acting Under Secretary for Technology
NATIONAL INSTITUTE OF STANDARDS AND TECHNOLOGY, Raymond G. Kammer, Director

National Institute of Standards and Technology Technical Note
Natl. Inst. Stand. Technol., Tech. Note 1398, 40 pages (May 1998)
CODEN:NTNOEF

U.S. GOVERNMENT PRINTING OFFICE
WASHINGTON: 1998

For sale by the Superintendent of Documents, U.S. Government Printing Office, Washington, DC 20402-9325

CONTENTS

PORTABLE CALIBRATOR FOR ACROSS-THE-ROAD RADAR SYSTEMS

Arthur R. Ondrejka and Robert T. Johnk

Electromagnetic Fields Division
National Institute of Standards and Technology
Boulder, Colorado 80303

The calibrator provides simulated radar reflections with a choice of target signatures, such as automobile, truck, small vehicle like a motorcycle, and several trucks in close proximity, to test those radars that have the ability to distinguish these targets. The calibrator can also simulate a vehicle approaching or receding from the radar in order to evaluate the radar's effectiveness in differentiating the direction of target motion.

This paper describes an inexpensive, easy-to-use electronic calibrator that can be used to improve the credibility of across-the-road type radars. Such a device can detect actual failures that generate erroneous speed readings. Regular documented use of the calibrator can greatly facilitate the maintenance of across-the-road systems by indicating faulty readings and trends in the radar operation, indicative of imminent failure. A precision calibrator is necessary to determine that the radar instrumentation is operating properly and that the computer algorithm results in displaying the correct speed.

Key Words: across, antenna, accuracy, beam width, calibrator, chirp, Doppler, Fourier, photo, radar, switch, transmission, verification, uncertainty.

1. INTRODUCTION

An electronic calibrator for evaluating across-the-road radars has recently been designed and developed by the Electromagnetic Fields Division at the NIST Boulder laboratories. The purpose of this calibrator is to provide a precision standard reference signal for the verification of radar units. This type of radar has been used extensively in Europe since 1974 [1], but is only now being considered for introduction into the United States. Even though modern across-the-road systems are basically a CW Doppler radar, these systems are significantly different from the older, down-the-road radar guns, which have to be aligned with the direction of motion of the moving target vehicle. Across-the-road radar transmits energy into a very narrow beam that is positioned at an angle with respect to the road. The speed measurement occurs when a target vehicle passes through the radar beam. The fact that measurements are no longer being taken with the target vehicle traveling parallel to the main radar beam introduces problems into the speed measurement system that require a careful daily calibration to

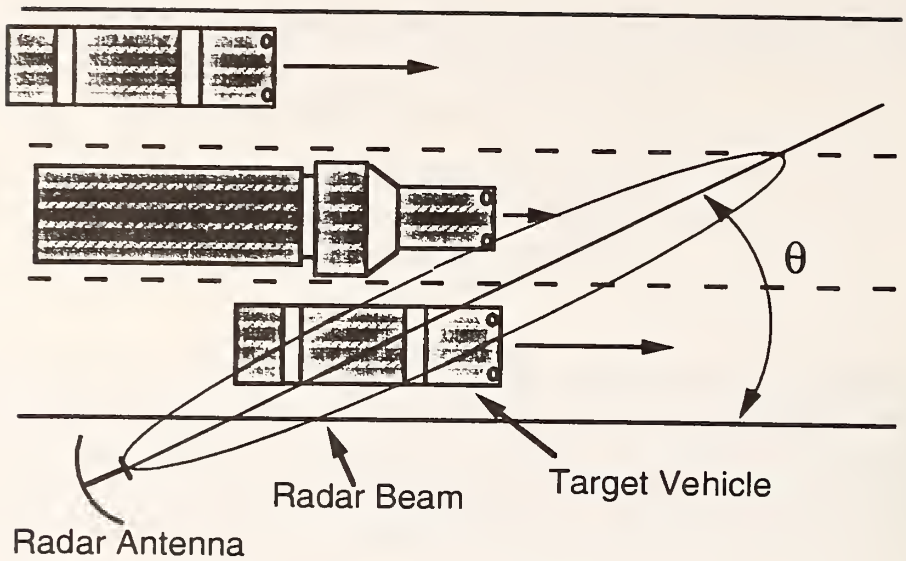

Figure 1. The across-the-road radar concept.

guarantee the accuracy of an across-the-road system. This paper describes an electronic device that can be used for this purpose. The simple architecture of this calibrator makes possible low-cost mass production using printed circuit board techniques.

Across-the-road radar systems have several advantages over the more familiar down-the-road systems. Perhaps the most salient is the ability to provide positive identification of offending vehicles by providing a license plate photograph of an offending vehicle. Also, across-the-road systems can be operated in the automatic, unattended mode, thereby freeing law enforcement personnel. Across-the-road systems can register up to 260 offenses per hour, a capability that cannot be matched by older down-the-road radars or the newest state-of-the-art lidar systems [9]. Also, since the radar beam energy is not directed down the road, detection by personal radar detectors is a much more difficult. Thus, across-the-road systems possess stealth capabilities that conventional down-the-road systems simply do not have [1].

A significant disadvantage of across-the-road radars is slightly reduced accuracy. When these radars are used correctly, their speed accuracy is generally ±2 mph at 55 mph. A properly used down-the-road radar gun can determine vehicle speed to well within a ±1 mph uncertainty. Future requirements may be as restrictive as +1, –2 mph at maximum speed (say 120 mph). However, the percent accuracy is relatively constant at different speeds. A –2 mph error at 120 mph is a –1.7 percent error. This same percentage at 55 mph gives a –0.9 mph error. An error limit of +1, –2 mph is pushing the normal capability of the radar system, so the radar will have to be calibrated often. We have designed our calibrator to make this operation easy.

The concept of an across-the-road radar system is depicted in Figure 1, where the radar is placed at the side of a thoroughfare and the radar main beam is aimed at an angle θ with respect to the direction of motion of traffic. A target vehicle traveling at highway speeds passes through the beam very quickly, usually in less than a second. The radar system must make a correct measurement of the vehicle's speed quickly, as well as compensate for both the error caused by the angle of the radar beam and the variation in the Doppler-shifted frequency as the vehicle moves through the various angles of the beam. This change or chirping of the Doppler frequency is called the cosine effect [1,2,3,4] since the frequency is a function of the cosine of the angle between the direction of target motion and the radar beam.

The Doppler-shifted frequency is given by

$$f_{Doppler} = f_r \pm f_d = f_r \pm \frac{2 f_r v}{3 x 10^8} \cos(\theta) , \quad (1)$$

where v (m/s) is the speed of the target vehicle, f_r (Hz) is the transmitted frequency of the radar, f_d is the Doppler shift, that is, the difference between the Doppler-shifted frequency and the transmitting

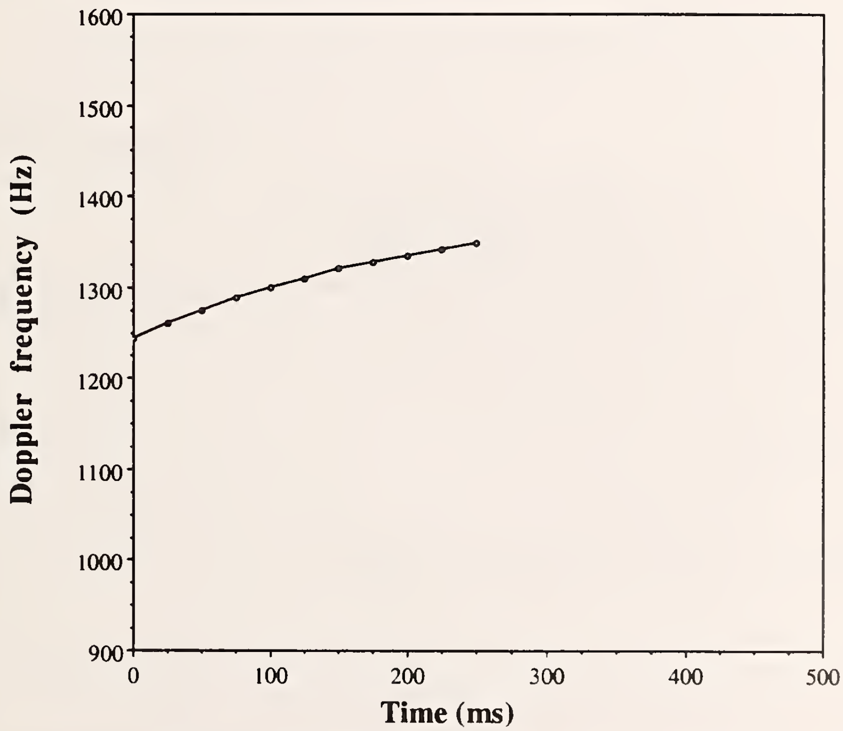

Figure 2. Calculated Doppler frequency from eq (1) for a spherical reflector passing through an across the road radar beam at 20 mph. Note the upward chirp in the Doppler shift indicates that the target is moving away from the radar.

frequency, and θ is the angle between the direction of the traffic flow and the main beam maximum. The term "Doppler frequency" is sometimes used instead of Doppler shift in the literature. The plus sign in Eq (1) denotes an approaching target with an upward Doppler shift, and a minus sign corresponds to a downward Doppler shift due to a receding target. Equation (1) would be exactly true if the target were a small reflector like a sphere with only one scattering center located at a point. The change in Doppler frequency due to the cosine term in Eq (1) is depicted in Figure 2, where an upward chirp for a receding target has been plotted. However, since all motor vehicles possess complex, distributed geometries, as is depicted in Figure 3, various portions of a target vehicle will pass through the main radar beam at different times resulting in a complicated spectrum of overlapping Doppler chirps in rapid succession. This sequence of signals is unique for a given type of vehicle and is called the vehicle's signature [1,5]. Figure 4 shows the complexity of the measured Doppler spectrum that was detected by an across-the-road system during actual field measurements obtained here at NIST. The target vehicle was a pickup truck passing through a radar beam at 20 mph. Figure 5 shows the same data after averaging. The chirps correspond to the intervals of rapidly rising frequency, and there are three distinct chirps visible. Across-the-road systems must process vehicle signatures that are far more complicated than those obtained for the older down-the-road systems. This makes it necessary to have a calibrator to establish their accuracy.

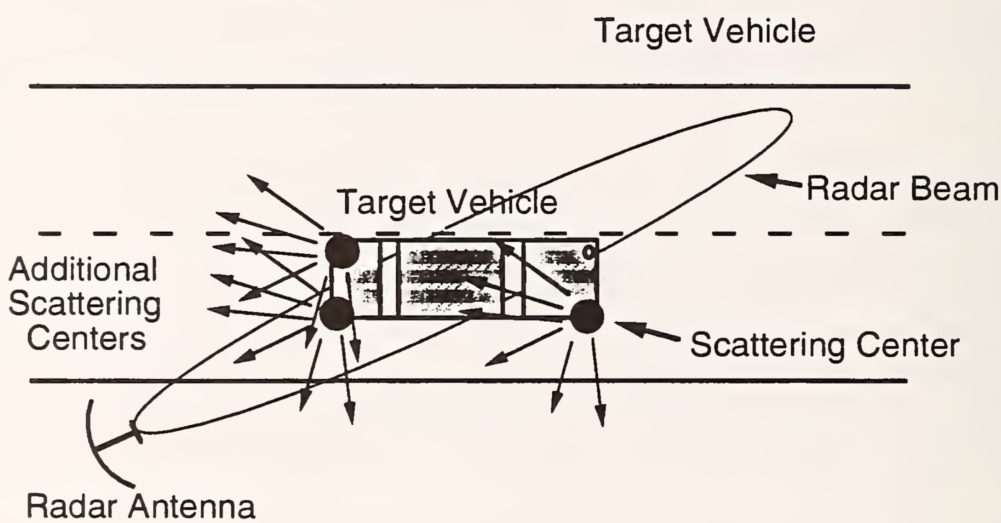

Figure 3. Multiple scattering centers of a target vehicle.

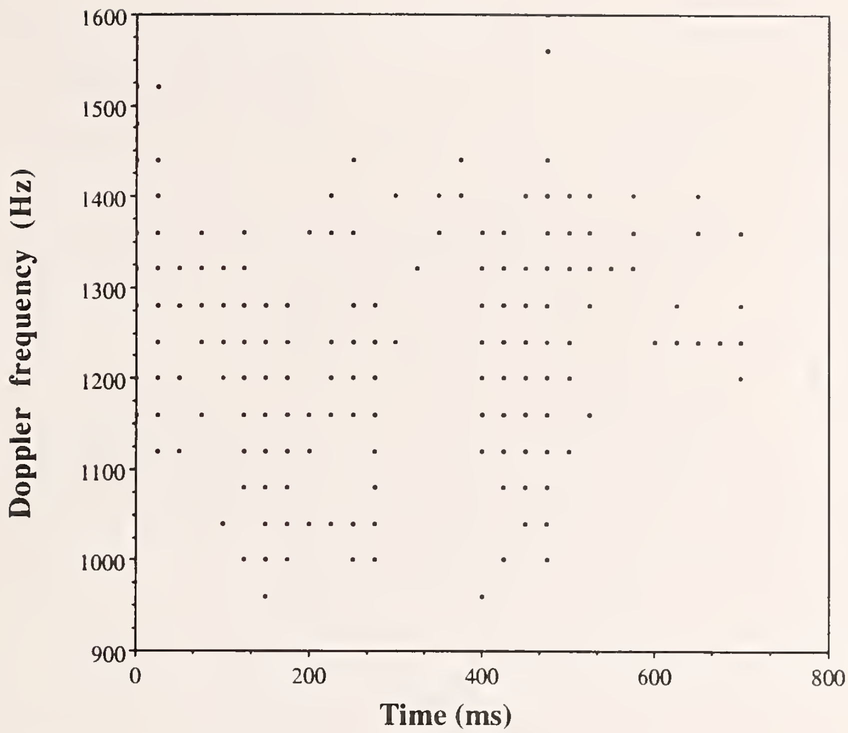

Figure 4. Measured Doppler frequency spectrum for a small pickup truck passing through a radar beam at 20 mph. The time interval for each measurement is 25 ms.

2. DESCRIPTION OF ACROSS-THE-ROAD RADAR SYSTEMS

The block diagram in Figure 6 shows that the across-the-road radar system is composed of a low-power CW generator that transmits a continuous wave of microwave radar energy in one of three microwave bands, an antenna to focus the energy into a narrow beam, a receiver that senses the microwave energy that is reflected from the target vehicle and measures the Doppler shift between the transmitted energy and the returned reflection, and a computer that processes the received signal to determine the speed of the target vehicle. An optional camera which can photograph the target just as it emerges from the radar beam may be included [1,6]. Three microwave bands are allocated for the operation of across-the-road radar systems Table 1 gives the band, the range of carrier frequencies, and a representative range of the Doppler shifts for a vehicle speed of 55 mph, and <u>when the carrier frequency is exactly at the middle of the band</u> [7].

The chirp frequencies are given as an example only. The exact range of frequencies must be calculated for each radar carrier frequency using eq (1). The calibrator being described was designed for the K-band units, but an appropriate calibrator can be built for any radar band.

The radar antenna plays a vital role in the operation of an across-the-road radar system. The function of

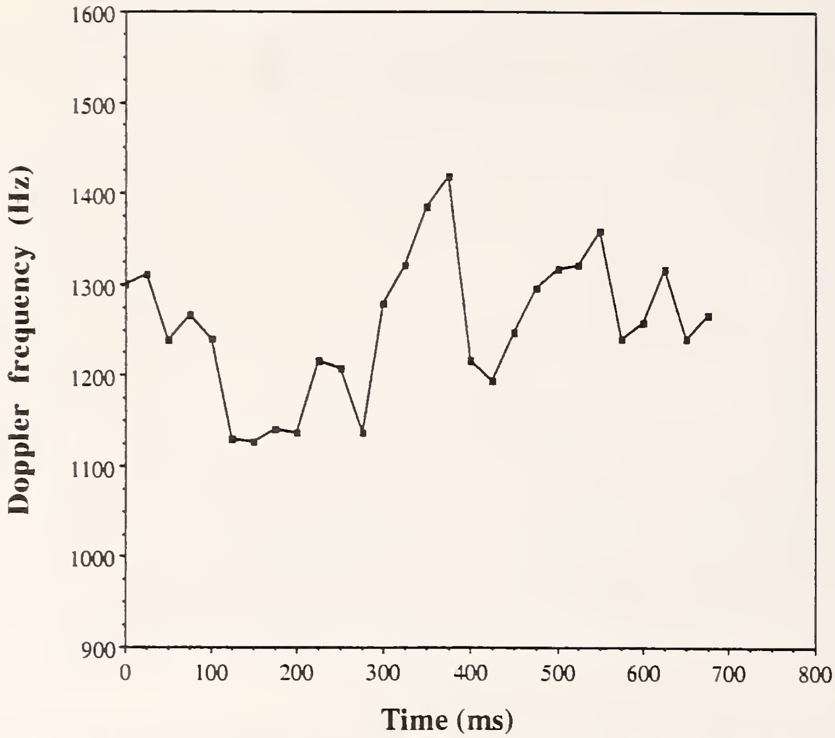

Figure 5. Weighted averages of the measured Doppler spectrum for the same pickup truck. Each point is averaged over a 25 ms intreval.

the antenna is twofold: it enables the radar to discriminate spatially between various vehicles; it also provides gain that boosts the reflected signal to a level that enables accurate and efficient processing. Several different antenna types are used on these radar systems: parabolic dish antennas, pyramidal horn antennas, and slotted array types. While horn and parabolic dishes are the most familiar types, slotted arrays are conformal, rugged, and amenable to gain pattern adjustment [8].

The CW generator on across-the-road systems is typically a Gunn diode oscillator that generates power on the order of 100 mW. These sources generate clean sinusoidal signals that are quite suitable for use in CW Doppler radar applications [7,8], and the power is more than sufficient to obtain accurate speed data for the short measurement distances that are involved.

Table 1. Doppler shifts for selected radar bands.

Band	Carrier frequency range (GHz)	Doppler frequency chirp (Hz)
X	10.50 – 10.55	1564 – 1667
K	24.10 – 24.25	3592 – 3828
Ka	33.40 – 36.00	5156 – 5495

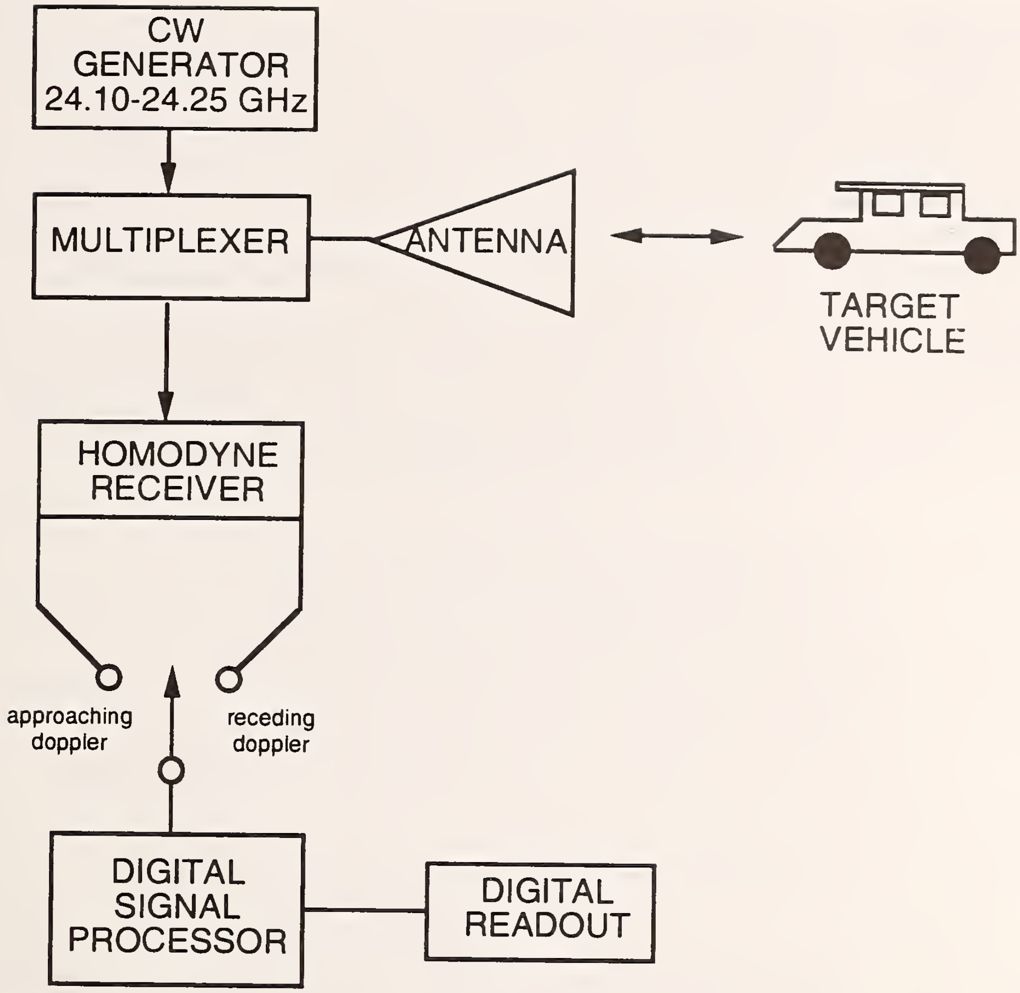

Figure 6. Block diagram of an across-the-road radar system.

The most complex and expensive component of an across-the-road system is the receiver. It must not only be capable of measuring the speed of the target vehicle but also must be able to discriminate between vehicles that are approaching from those that are moving away from the antenna. For this purpose, the receiver must have the ability to determine whether the Doppler-shifted frequency is higher or lower than the transmitted signal, which requires a sophisticated filtering or a sideband cancellation scheme [7,8]. Furthermore, since the speed limits for trucks are sometimes different than automobiles, the radar must also be able to identify the type of vehicle in its beam. Such a capability is implemented by measuring the amount of time that a selected target vehicle is in the radar beam.

3. DESCRIPTION OF CALIBRATOR

The operational concept of the NIST-developed calibrator is depicted in Figure 7. The calibrator receives the transmitted radar signal and directs it to a switched passive delay line which, in turn, modulates and reflects the signal back to the radar under test. The switching sequence is precisely controlled so that the reflected signal is modulated in a manner that is very similar to that of a passing vehicle. The reflective phase shifter circuit that is realized in this manner mimics a vehicle passing through the radar beam and provides the basis for an accurate calibration standard. The reflective switch principle results in a one-port architecture that is simple and easy to implement using printed-circuit board techniques, suitable for low-cost mass production. Thus, it might very well be cost effective and economical to incorporate a printed circuit version of the NIST calibrator into all operational across-the-road systems for on-site performance verification.

For actual radar system calibrations, the signal generated by the calibrator should cause the radar to read a speed of 55 mph for several categories of vehicles (cars, motorcycles, trucks) that are either approaching or receding from the radar. Since the speed indicated in the readout on the radar unit cannot be adjusted by the operator, the results of these tests are simply recorded for future reference. If the speed readings are outside the error limits set by the user, the operator may add or subtract the

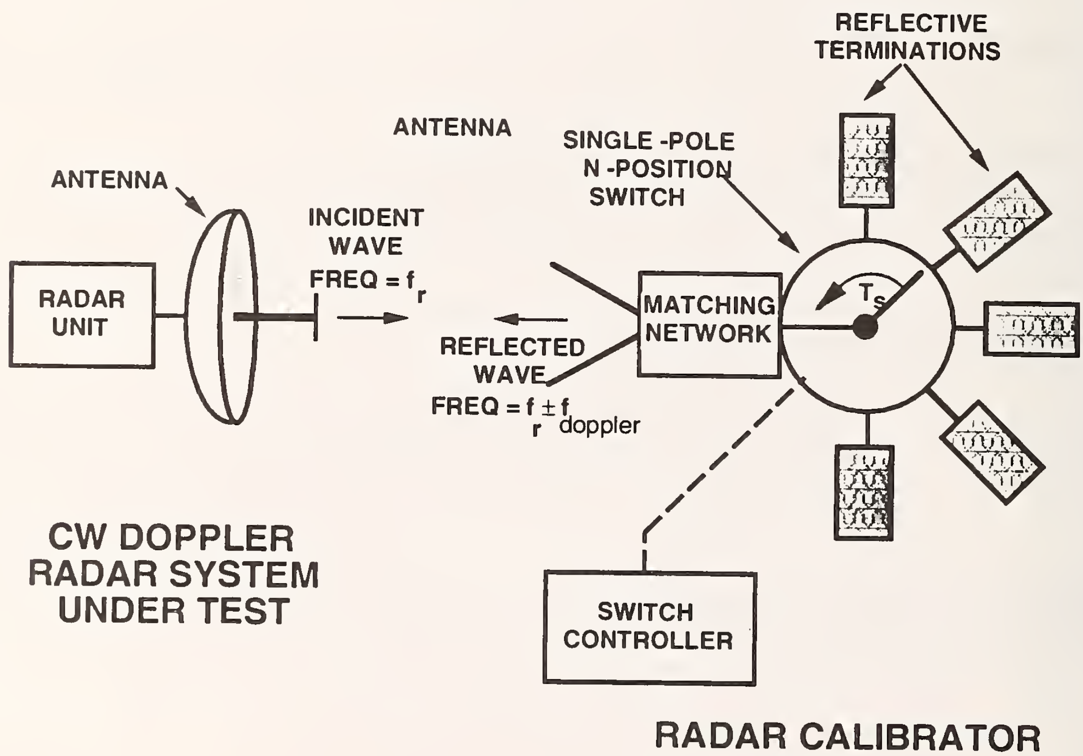

Figure 7. The NIST radar calibrator concept.

offset difference to the actual speed readings to correct the measurements in real traffic. This is tedious. Furthermore, the operator is warned that the unit may be marginal and approaching a condition of more serious errors. Under these conditions, it is recommended that the radar unit be returned to a service depot for repair and readjustment.

The calibrator, the details of which are to be described, can be enclosed in a volume less than 15 cm on a side and weighs less than 1 kg, including batteries. The operation of the NIST calibrator is straightforward. In use, it is placed in front of the radar unit and provides a synthetic reflected signal each time a switch labeled "Calibrate" is depressed. It simulates a Doppler signal which is similar to that produced by an actual target vehicle traveling at 55.0 mph ± 0.1 mph. It approximates the information of the cosine variation in Doppler frequency and provides a selection of durations of the signal to simulate a motorcycle, automobile, truck, or cluster of several vehicles. Furthermore, it can shift the radar's microwave frequency up or down depending whether it is simulating an approaching or receding vehicle.

The required horizontal beamwidth for an across-the-road radar is 5°. This is a measure of the intensity of the radiated power density as a function of angle from center of the radar beam (boresight). For a 5° beamwidth, the power density in the beam decreases to half the boresight power at ±2.5°. The pattern amplitude decreases to a small value at ±5°. The NIST-developed calibrator is designed to chirp the entire ±5°, which is equivalent to sweeping from 53.0 mph to 56.5 mph, on the upward chirp. There are two normal combinations for the calibrator: either the reflected microwave frequency can be higher than the one transmitted by the radar, as if the target were approaching, and the frequency is swept (chirped) downward toward lower frequency, or else the reflected frequency is lower than the radar, and the chirp is upward, as for a receding target. If the radar is set to detect approaching targets and the calibrator is set for the receding combination, the radar should reject the signal entirely.

The calibrator is intended to be used for six routine tests which are done at the speed measurement site before and after each day's use of the radar. Results of these tests are usually recorded in the radar operator's log for future reference. These six tests include the Doppler audio test, speed calibration, vehicle type discrimination, direction separation (approaching and receding vehicles), radar system sensitivity, and EMI compatibility with the other electrical and/or electronic systems which might be located in the radar vehicle.

4. OPERATION AND DESIGN

Figure 8 shows a typical calibrator with an exploded view showing the major components. A Teflon radome covers the aperture of the microwave horn antenna and provides protection from the environment without significantly impeding the microwave energy from the radar unit. An aluminum shield around the antenna prevents radar energy from leaking past the antenna and interfering with the operation of the control circuits. The printed circuit board mounted against the back wall of the enclosure contains all the associated circuitry needed for operation of the calibrator.

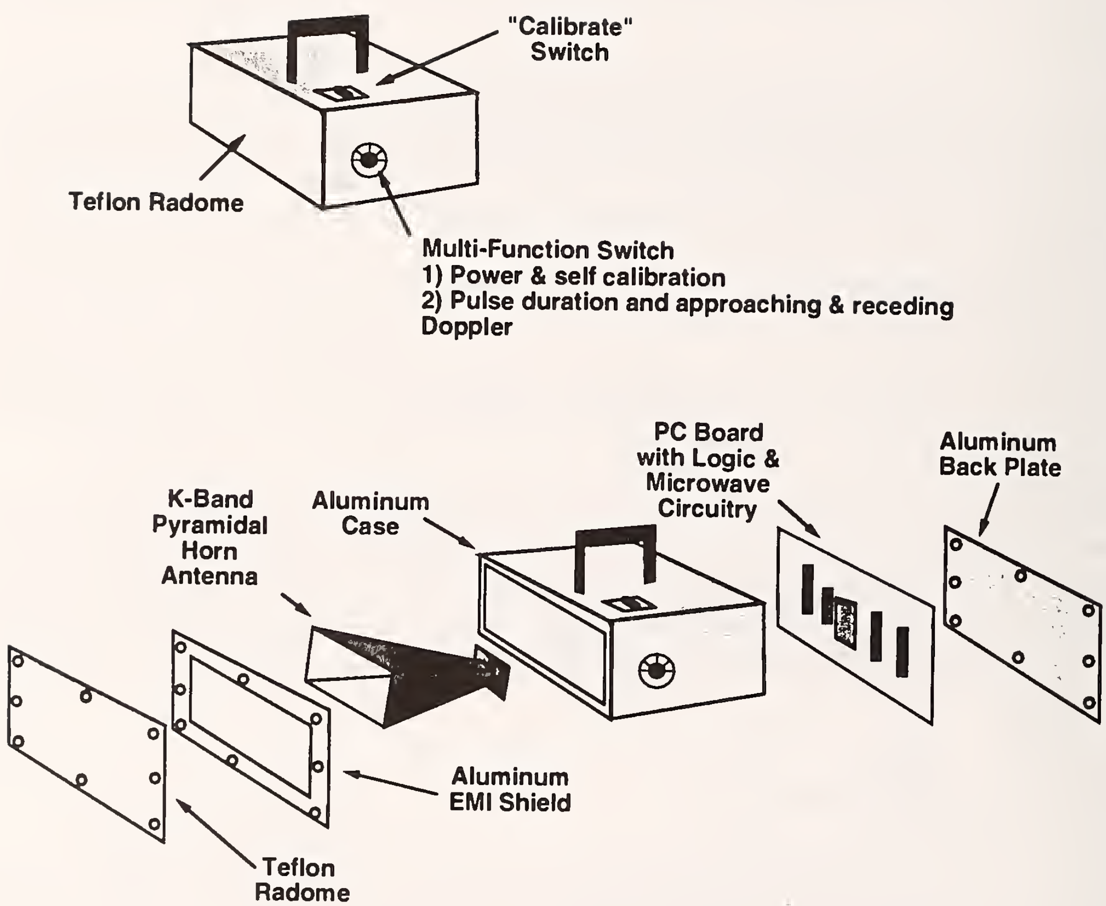

Figure 8. Drawing of the NIST calibrator with an exploded view.

A momentary switch (labeled "Calibrate") located near the handle on top of the calibrator initiates each reflected signal. The switch located on the side of the box turns the power on and selects the particular type of operation desired, that is, auto or truck, approaching or receding, and chirp upward or downward. Several other options include various self tests and radar diagnostics.

Figure 9 shows a detailed block diagram of the calibrator. The architecture of the calibrator consists of two main functional units: the microwave switch section and the switch control section. The switch section consists of an antenna, a single-pole five-position switch, and a matching network. The switch control section contains low-frequency electronic circuitry that generates precisely controlled signals which drive the switch to a number of prescribed sequences. The selection of a sequence is determined by the particular test that is being performed on a given radar system.

Basically, the device is a modulated passive reflector. The CW microwave energy from the radar is received by the calibrator antenna, reflected from the open circuit end of the switched delay line, and re-emitted toward the radar unit. The information carried by the reflected signal is determined by the way the switch is sequenced. In each successive switch position, the delay line is a little longer so that the microwave energy has further to travel, giving a reflected signal which seems to be coming from an object that is moving away from the radar. Eventually, the switch must return to its starting position, but this simply moves the waveform backward by 360° with no noticeable interruption in the Doppler shift. The overall effect is that of a continuously receding vehicle. Of course, the switch can be sequenced in the reverse order giving the effect of an object approaching the radar. One complete sequence of the switch generates one cycle of the Doppler frequency. The switch rate is continuously increased or decreased in constant increments to simulate the desired chirp. A detailed mathematical analysis of the calibrator operation is presented in Appendix A.

In the microwave section of the calibrator, only the antenna, switch, and delay lines operate at the K-band frequencies, simplifying the microwave circuitry. For a commercial version, we anticipate that these three components will be fabricated onto a single microwave printed circuit board substrate. In our present breadboard, the antenna used is a K-band standard gain horn using a precision 2.92 mm adapter. The switch is a commercially available single-pole, five-position, coaxial diode switch which was originally designed for use up to 18 GHz. As Figure 9 shows, the matching network consists of a shunt-connected tuning stub located at the switch input to lower its input VSWR at the operating frequency of 24.15 GHz. The shunt stub consists of a coaxial tee connector to which is connected an open ended length of 0.141 in diameter coax line. This would probably not be necessary if the switch were designed for use at K-band. Since the switch is coaxial, we designed the delay lines from short lengths of the same coaxial cable as the tuning stub. Unfortunately, the switch was manufactured with SMA connectors on all ports, so all stubs had to follow suit, and because of the interacting effects of all the connectors, the whole combination had to be modeled on a linear microwave network simulator to optimize it properly. A single substrate commercial unit would be much simpler and very inexpensive. Such an integrated microstrip architecture would be much easier to produce and it would perform much better. The process and procedures for designing the microwave switch section is discussed in detail in Appendix B.

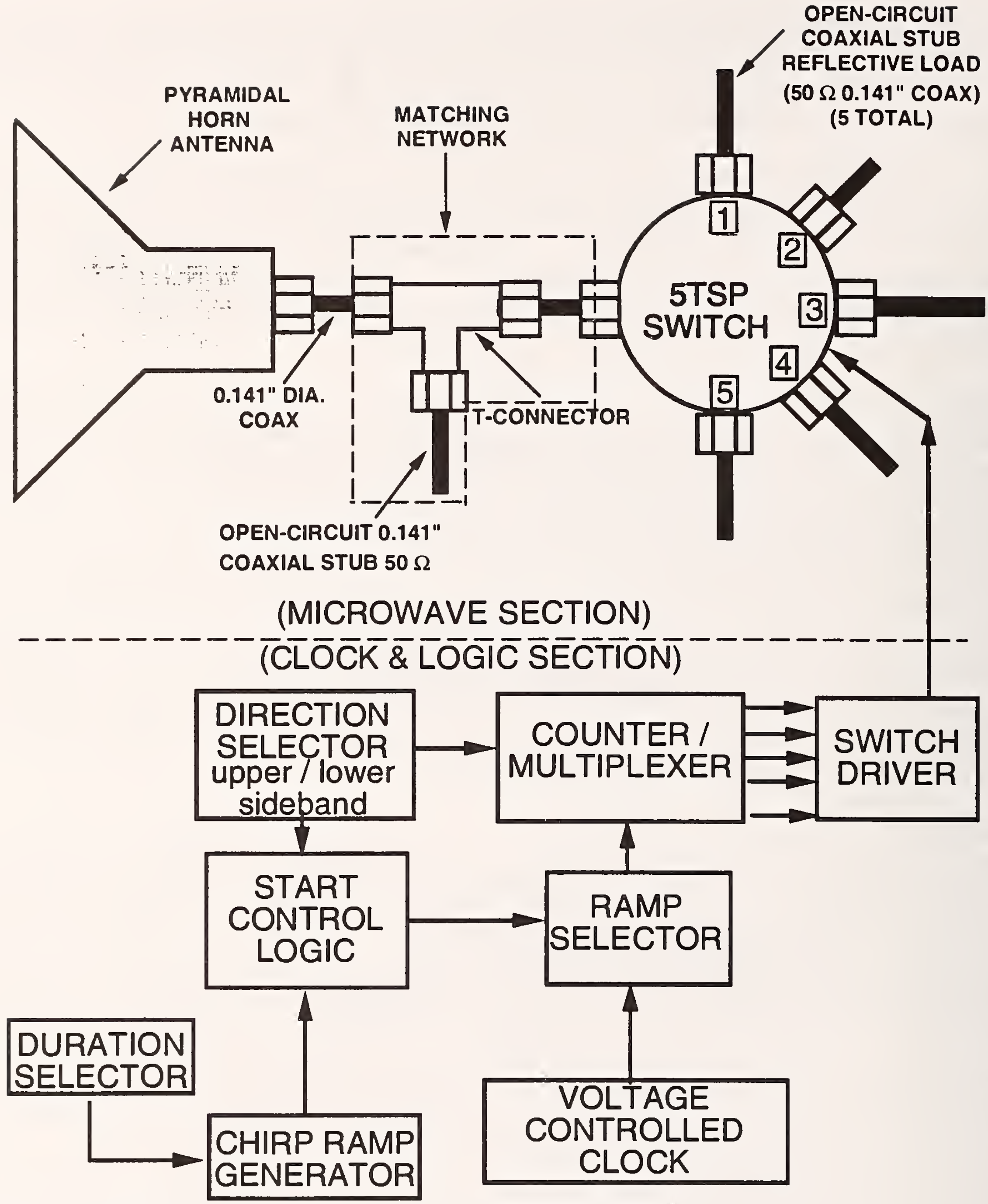

Figure 9. NIST radar calibrator system block diagram.

5. SWITCH CONTROL SECTION CIRCUIT OPERATION AND DETAILS

The remaining circuits are necessary to drive the switch and are located on a separate circuit board. This section contains clock circuits that provide the signals that step the switch and the precision ramp voltage that sweeps the clock frequency upward or downward. The clock frequency and the ramp voltage will drift for several minutes after the calibrator is turned. In order to stabilize these critical circuits and avoid the problems associated with drift, they are allowed to free run and generate a Doppler shift which is continuously being chirped first upward and then downward. This sequence is not interrupted by a request for an output. When the operator initiates a reflection sequence by depressing the "Calibrate" switch, the logic circuit selects one of the ramps as directed by the operator.

The chirped clock signal activates a simple ring counter which can be stepped from low bit to high bit or vice versa. This determines in which direction the switch will be sequenced, as an approaching or receding target. This process generates either an upper or lower sideband with respect to the radar carrier frequency and should not be confused with chirping. The remaining circuitry is necessary to trigger the logic sequence properly.

The operator can select four durations for the simulated signal, 0.1 s, 0.25 s, 1.40 s, and 2.1 s. These correspond roughly to length of time that various sized vehicles are actually in the radar beam if they are traveling at 55 mph. These times simulate a motorcycle, an automobile, a truck, and a combination of vehicles that are too close to resolve. The first and last durations are often outside the capabilities of the radar, which simply notifies the operator of an error condition and withholds a speed reading output. Clearly, these are at best approximate times since the radar beam becomes wider at greater distances and different automobiles have different lengths, both of which would affect the signal duration.

The calibrator can then be set to synthesize the chirp variation due to a vehicle passing through the radar beam either approaching or receding. At 55 mph and a 5° wide K-band radar beam centered at 20° to the line of approaching traffic, and for a carrier frequency of 24.175 GHz, we would expect the Doppler shift to chirp downward from 3828 Hz to 3592 Hz. This is not a linear sweep but a curved function determined by the cosine of the angle (see Eq (1)) between the direction of the vehicle and the direction of the radar beam. Often, radars make no use of the information in this curvature and presume a linear sweep. The calibrator is corrected for the slight difference due to the curvature.

Figures 10 and 11 are schematics of the actual circuits used for our prototype system. Figure 10 shows the system clock. It is adjusted to be five times the desired Doppler shift frequency, since our switch requires five positions per cycle of Doppler. The frequency of the clock is modulated by a triangular (ramp) waveform so that its frequency is alternately chirped upward and downward. The clock and ramp generators are two halves of a CMOS TLC556I depicted in Figure 10. In each part, the output square wave drives the RC timing circuit to produce the triangular ramp waveform. R1-C1 controls

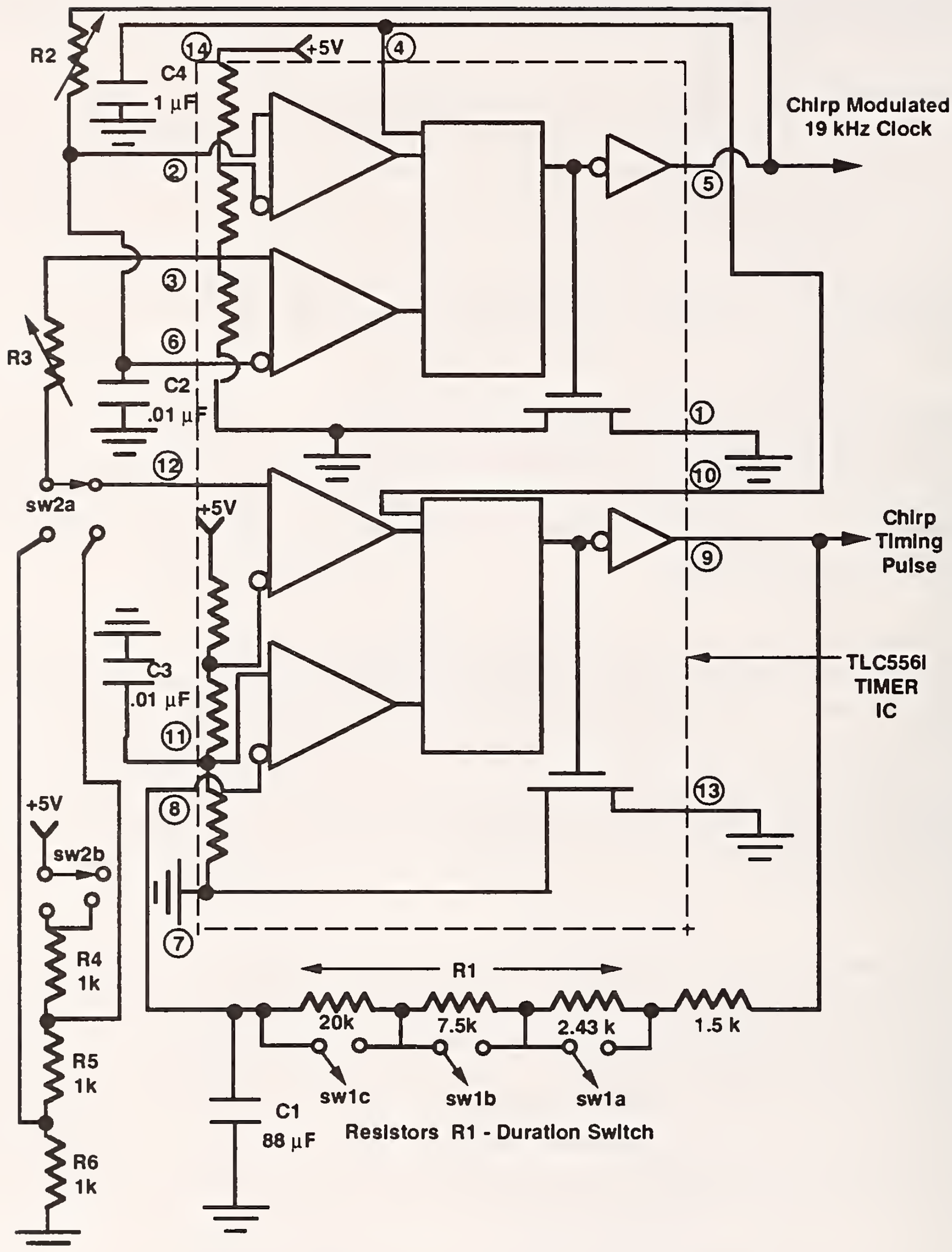

Figure 10. Clock signal generator circuit.

the pulse duration and the sweep ramp voltage. R2-C2 controls the 19 kHz clock frequency. R3 controls the amount of ramp voltage which is applied to the 19 kHz clock timer, therefore adjusting the amount of frequency chirp that will be produced. Switches SW 1a, 1b, and 1c, can be configured to select any of the pulse durations given in Table A of which only the four mentioned previously are actually used. Switches SW 2a and 2b select either the normal ramp modulation, or a high or low dc voltage which will produce a constant Doppler shift equal to, respectively, the high or low frequency limit of the chirp. The frequency of this unchirped signal can be measured using a precision counter, and if there are errors, the low frequency can be adjusted using R2. The high frequency can be adjusted using R3.

If the accuracy or stability of the clock and ramp circuitry is not adequate under all operating conditions, such as extremes of operating temperature, the clock can be replaced with a crystal-controlled device, and the ramp generator by a more precise digital circuit.

The Switch Driver in Figure 11 is a ring counter composed of a CD4015 dual shift register and associated logic circuits. The two registers are clocked in opposite directions, and one of these is selected to produce the effect of approaching traffic and the other for receding traffic. A high bit is introduced into the register and propagates through all four cells. Each of these logic conditions activates one position of the microwave switch. The fifth position of the switch is activated when all register cells are low (CD4002). The binary encoder was necessary only because the microwave switch we selected required binary coded inputs. This circuit may not be necessary for other switches. The microwave switch is a commercially available unit designed for use up to 18 GHz.

The remaining electronics in the lower portion of Figure 11 are logic control circuits. Since the clocks are free running, a randomly timed request from the operator to initiate a signal will rarely occur at the correct part of the clock cycle. In order to avoid generating a faulty signal, the circuit waits until it recognizes the end of the chirp cycle just before the correct one. Then the logic turns on the microwave switch at the beginning of the desired chirp. The circuit shown as Start Logic makes this selection.

The manual "Calibrate" switch, SW4, is normally in the reset position and the output from U26 is low. The operator begins a Doppler chirp by moving the switch to the Trigger position. The pair of Schmitt triggers form a switch debounce. If the chirp timing signal at SW5 is low (wrong chirp ramp in progress), the output of U19 goes high setting the flip-flop U23/24 high. U25 then waits for the chirp timing signal to go high before allowing an output, and the timing cycle is correct. All later repetitions of the chirp timing pulse are excluded from the output until flip flop U17/18 is reset by returning switch SW4 to its Reset position.

If the chirp timing signal is already high (desired chirp ramp is in progress) when switch SW4 is triggered, taking an output from the ramp generator would produce only a portion of the ramp. Therefore, the logic waits until the previously described sequence takes place. The high input to U19 keeps its output low which retains the output of U23/24 low, and the logic output stays low. When the chirp timing signal goes low, the output of U19 goes high, switching U23/24 output to high setting

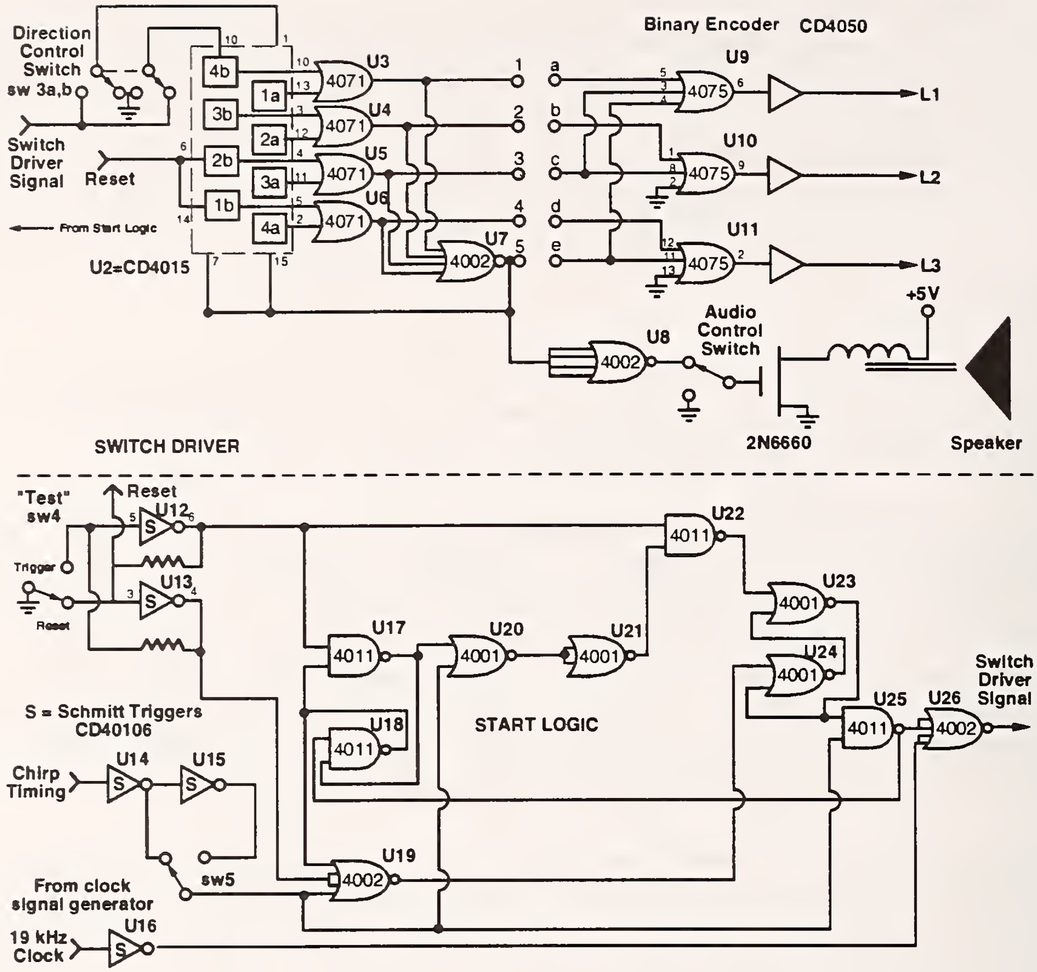

Figure 11. Schematic diagram of the switch driver and control logic.

with U25 ready for the next high from the chirp timing logic. As soon as this high appears (correct chirp ramp), the output of U25 goes low, turning the logic on and delivering the 19 kHz chirp to the switch driver circuit.

6. LABORATORY TESTS ON THE CALIBRATOR

The spectral content of the reflected calibrator signal was obtained using the simple laboratory test setup of Figure 12. The test setup consisted of a CW microwave synthesizer, a 20 dB waveguide directional coupler, a WR-42 waveguide pyramidal horn antenna, and a microwave spectrum analyzer. This setup provides a direct measure of the signal content that is reflected by the calibrator and thereby an assessment of the calibrator performance. In this test, the calibrator was switched at a constant rate with an equal time allocated to each of the switch positions. In Figs. 13 and 14 the signal at the center of the spectrum analyzer trace is the radar transmitter output (carrier) which was chosen to have a

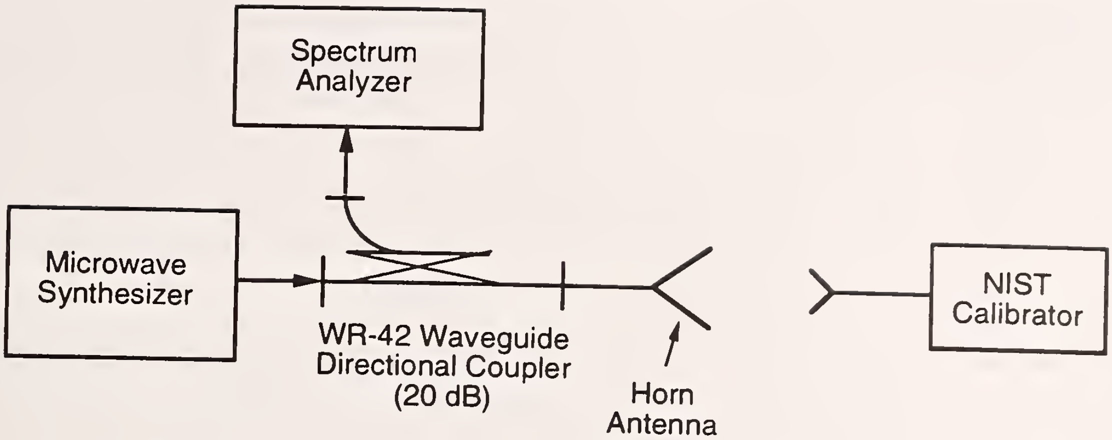

Figure 12. Laboratory setup for the calibrator performance test.

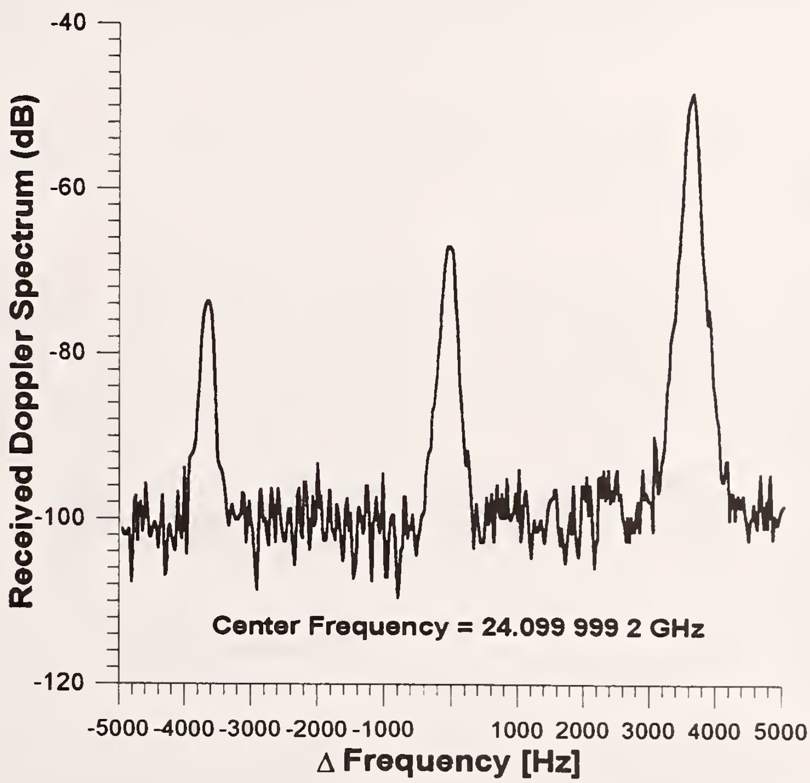

Figure 13. Measured spectrum obtained from the NIST calibrator for an increasing phase sequnce with $1/T_s = 3620$ Hz. Note that the dominant reflected spectral component is 3620 Hz above the synthesizer transmitting frequency of 24.10 GHz.

frequency of 24.10 GHz. The signals that are located ±3620 Hz on either side of the carrier are the Doppler-shifted sidebands produced by the calibrator. This is the correct Doppler shift for the original simulated speed of 55 mph. If 65 mph would be a more appropriate speed, the correct Doppler shift would be 4670 Hz. The calibrator is set in the "test" mode where the chirp generator is de-activated, and the output is a continuous signal. The upper curve (Figure 13) shows the resulting frequencies when the calibrator is set to simulate an approaching vehicle. The dominant signal is the upper sideband frequency which is clearly 20 dB greater than the reflected carrier. The undesired lower sideband is suppressed 25 dB below the desired one. The lower curve (Figure 14) shows that the reverse is true when the calibrator is set for a receding vehicle.

The suppression of the undesired sideband is a function of several parameters, but principally it is determined by the number of positions in the microwave switch. A Fourier series analysis of the switched delay line signal indicates that a four-position switch would provide about 16 dB suppression, which we decided would be inadequate. A five-position switch provided a significant improvement of an additional 9 dB. A six-position switch would involve higher cost with only slight performance improvement over the five position switch. The five-position switch was chosen as the practical compromise. A Fourier series analysis of the switch is presented in Appendix A.

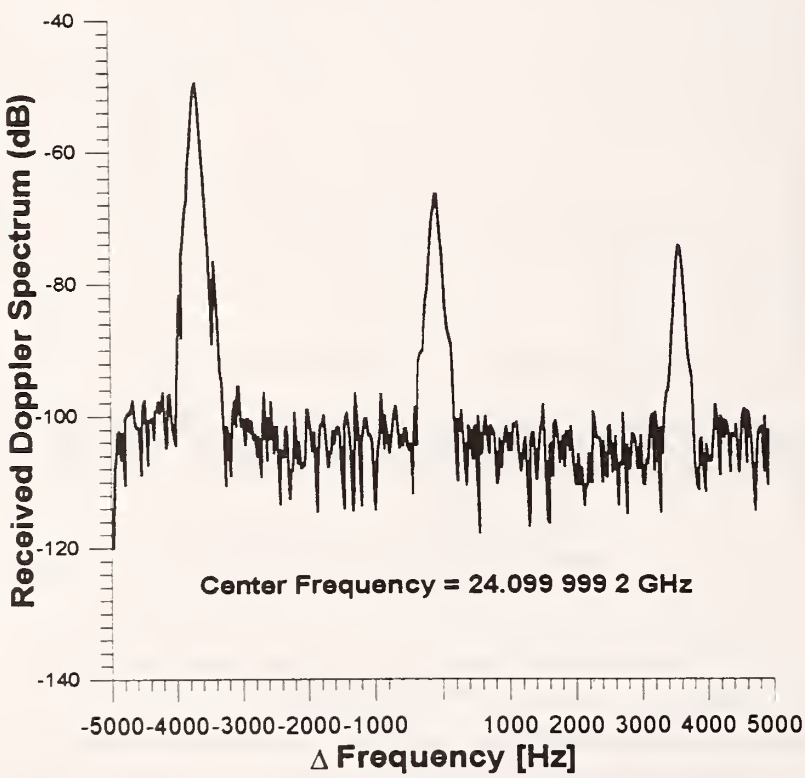

Figure 14. Measured spectrum obtained from the NIST calibrator for an decreasing phase sequnce with $1/T_s = 3620$ Hz. Note that the dominant reflected spectral component is 3620 Hz below the synthesizer transmitting frequency of 24.10 GHz.

The other parameters that should be considered are those that affect the amplitude of the reflected signal. Therefore, the switch should be chosen to have a minimum change in input reflection coefficient amplitude and insertion loss between switch positions.

7. RECOMMENDED TESTS FOR ACROSS-THE-ROAD SYSTEMS

These tests, classified as Field Calibrations, are intended to evaluate those parameters of an across-the-road radar system that have a direct and significant effect on the accuracy of the radar unit, and which have the greatest possibility of changing from day to day. It is recommended that they be performed daily. Five tests can be performed simultaneously by this procedure: audio output, speed calibration, direction sensing, radar sensitivity, and EMI susceptibility. Errors in the angle of the radar beam due to misalignment of the radar vehicle with the direction of traffic can not be measured by this calibrator.

A Audio Output. An audio-frequency output of the Doppler shift is available on many commercially available radar systems. This may be produced either by a calibrator or any vehicle passing through the radar beam. During this test, the sound intensity can be adjusted to a level that can be heard comfortably in normal traffic noise.

B Speed Calibration. The radar should be tested for correct speed reading before and after use in traffic using the precision electronic calibrator. The ideal displayed speed for this calibrator is 55.0 mph.

C Direction Sensing. The direction sensing circuits should have at least 20 dB rejection of the undesired direction compared to the desired one. This should be tested before and after use in a traffic condition. The speed test cycle is repeated using the electronic calibrator set to synthesize an approaching vehicle while the radar is set to detect a receding one. The radar should reject the signal giving a reading of either 0 mph or ERROR. The other combination of synthetic receding vehicle and approaching direction in the radar can also be verified.

D Radar Sensitivity. The radar's sensitivity is measured by the greatest distance over which it can make a correct speed measurement. This "initial detection range" can be tested daily as part of the setup procedure using the electronic calibrator. The calibrator output is adjusted to a signal strength which is small, but one which the radar should be able to measure accurately. The radar can be tested further by moving the calibrator from its normal position of 2 m in front of the radar antenna to 6 m. This effectively reduces the reflected signal by about 10 dB, which is approaching a value that is too small for the radar the measure. Success in measuring this signal indicates that the radar is functioning at maximum sensitivity. Failure in this test does not disqualify the radar, but may warn the operator to expect continued decrease in the radar's effectiveness.

E Susceptibility to Radiated EMI. The radar must continue to operate when exposed to the normal fields that occur within the radar vehicle during operation of accessory equipment such as on-board or personal transceivers. These tests can be done while the calibrator is positioned for testing the radar. Each transmitter can be turned on for the duration of one calibrator test cycle. Clearly, the radar should still read the correct speed. If problems occur, the test indicates that, first, the particular transmitter should not be activated during radar operation, and second, that some type of maintenance is required to avoid the problem in the future.

8. DESCRIPTION OF TESTS PERFORMED

A commercial radar unit was chosen to test the effectiveness of our calibrator. This radar operated in the K band at a fixed frequency of 24.15 GHz. It was composed of a control unit with a separate microwave generator/antenna unit. The control unit contained the switches necessary for the operator to direct the functioning of the radar, such as whether it should sense automobiles or trucks, approaching or receding, close or far. It also was used to input the information about the current speed limits for autos and trucks. This unit contained the computer which calculated the speed of the target from the Doppler frequency, and determined when a violation occurred.

The generator/antenna unit produced the CW microwave signal, radiated it into a 5° wide beam, and received the reflected signal. This unit also processed the signal to determine whether the target was approaching or receding. The associated camera/flash unit was not included in the NIST tests.

The radar unit was set up in its standard configuration with its own internal calibrator connected between the antenna unit and the radar unit. This internal calibrator injects a Doppler-shift frequency directly into the low-frequency audio section of the radar unit without passing through the antenna or any of the microwave circuitry. It has a constant (not chirped) Doppler frequency which simulates a target vehicle traveling at 37 mph. This internal calibrator was activated many times during the tests and always gave the same response of 37 mph.

<u>For these tests, the NIST calibrator was set to generate a Doppler signal appropriate for a speed of 55 mph</u>. It was located directly in the beam of the radar under test, and 2 m away from it. The operator adjusted the calibrator controls for the proper test sequence, for example, truck approaching, and activated the start switch. Within a few seconds, the calibrator produced the required reflected signal and a speed reading appeared on the radar display. With both the calibrator and the radar preset to detect approaching trucks, for example, the radar should read 55 mph ± 1 mph. When the radar was preset to detect any improper combination of vehicle and direction, it should have read either 0 mph or ERROR.

There were several switch options on the front panel of the radar unit that are listed in Table 2.

There were several indicator lights on the radar front panel including a power on, a battery condition, and a signal present. This last indicator remained lit only as long as a Doppler signal was being presented to the radar. At power up, the radar made some critical self tests and proceeded only after it had passed the tests.

Table 2. Switch options on the front of the radar unit.

Switch option	Function
a	target approaching, receding, or both
b	target automobile, truck, or both
c	automobile speed limit input
d	truck speed limit input
e	radar range setting I or II
f	radar reset switch which sets the speed readout to 00 mph
g	power switch

Table 3. Test results on a commercial across-the-road radar system.

Radar operational mode	Pulse duration	Signal recorded?	Speed recorded	Offense recorded?
Mode 1: Calibrator receding - Radar receding Automobile mode - Chirp up				
	0.1 s	Yes	0	No
	0.25 s	Yes	56	Yes
	1.35 s	Yes	56	No
	2.00 s	Yes	0--	No
Mode 2: Calibrator receding - Radar receding Truck mode - Chirp up				
	0.1 s	Yes	0	No
	0.25 s	Yes	56	No
	1.35 s	Yes	56	Yes
	2.00 s	Yes	0--	No
Mode 3: Calibrator approaching - Radar approaching Automobile mode - Chirp down				
	0.1 s	Yes	54	Yes
	0.25 s	Yes	55	Yes
	1.35 s	Yes	55	Yes
	2.00 s	Yes	56	Yes
Mode 4: Calibrator approaching - Radar approaching Truck mode - Chirp down				
	0.1 s	Yes	53	No
	0.25 s	Yes	55	No
	1.35 s	Yes	56	No
	2.00 s	Yes	56	No

We tested the radar for this power-on test and internal calibration with all combinations of these switch positions, and the unit passed all tests successfully. We then tested the radar for its ability to communicate with our calibrator, and discovered that its antenna was horizontally polarized. It communicated well with the calibrator located 1, 2, and 3m in front of the radar antenna. There was no communication when our calibrator was vertically polarized. We chose to continue the tests with a 2 m separation.

Using our calibrator, we tested the radar for accurate speed indication using all combinations of front-panel switch positions and all calibrator options. The range switch was tested in both positions for every combination of all the other radar switch options, but had no effect on the results. We surmise that the calibrator had adequate signal output to activate the radar at any range sensitivity, and these results will not be reported further.

The radar speed limits were set at 50 mph for both automobiles and trucks. A select few of these results are given in Table 3 below. The uncertainty of our calibrator at 55 mph is less than ±1% at laboratory temperature.

Notice the difference between the approaching mode and the receding mode. Also, notice the readings that appear as 0-- which indicate an error due to too long a pulse. This implies congested traffic where the radar may make an incorrect evaluation of speed, and, in the receding mode, no offense is recorded.

All measurements, where the approaching/receding modes on the radar and the calibrator were different, as, for example, having the approaching mode on the calibrator and receding mode on the radar unit, or vice versa, resulted in no input signal, that is, no signal indicator, and no speed readings on the radar output. This was true for all combinations of switch options on the radar and calibrator. This is an indicator of the quality of the calibrator's ability to reject the undesired sideband, which we reported previously to be 25 dB. This is adequate for our purposes.

Now considering the calibration data in measurement set 1, the radar was set to track only automobiles. The measured speed is 56 mph for chirp up. It appears that the data were taken at the end of the pulse when the vehicle was farthest away from the radar unit. The radar interpreted the 0.25 s pulse as an automobile and registered an offense since the speed was in excess of the 50 mph limit set into the radar. The radar also recorded no offense for the 1.35 s pulse since it interpreted it as a truck and the 2.0 s pulse, both of which it was supposed to ignore.

Data set 2 shows similar results for the radar switched to the truck mode. Offenses were recorded for the 1.35 s (truck) pulse, and the shorter pulses did not give an offense. Otherwise the error in the measured speed is similar to the automobile mode.

When the radar was set for approaching traffic, several differences were apparent. First of all, the radar did not wait until the end of the pulse to register its output. This implied to us that the radar was reading the data toward the beginning of the pulse. Data set 3 shows that when the Doppler frequency was chirped from high to low, the output speed was high. In other words, the measurement was taken early in the pulse when the vehicle was most distant. To confirm this conclusion, the calibrator was switched to its diagnostic mode and the approaching sideband was chirped from low to high. This combination is not found in normal radar use. The resulting speed reading was low, which confirmed the early-time hypothesis. These results would be consistent with the data in the receding mode if the manufacturer wanted to use only those data taken when the target vehicle was farther away from the radar. It certainly eliminates most of the complex target signature by making use of only the simpler reflection from the front or back of the vehicle and eliminating the complex reflections from the sides.

In the receding mode shown in data sets 1 and 2, since the radar took its data late in the reflection sequence, it was able to sense the duration of the pulse, and therefore to determine the length of the synthesized vehicle. With this information, the computer could properly assign the violation to either an auto or truck. In data set 3, since the measurements are concluding early in the reflection sequence, the radar set seems to be ignoring the length of the pulse, and it is clearly not discriminating between auto and truck reflections. A hazard in this procedure is that the radar is assigning a violation to all vehicle types. This is a serious system malfunction that was easily uncovered by the calibrator.

The synthesized truck data in set 4 resembles set 3 in that the speed reading is again being made at the beginning of the chirp while the frequency is high, and the radar does not discriminate between vehicle types. In this case, however, no violation is recorded for any pulse width. We propose that the radar set is not measuring the reflected signal for a long enough time to sense a truck. Data set 4 supports the claim that there is a serious malfunction in the radar unit and suggests that the set be returned to a repair depot for further diagnosis.

The variations of ±1 mph seem insignificant, but the average of the speed over this waveform was 55 mph, so the radar should have read the correct 55 mph. If the total allowable error is chosen to be +1, −2 mph, then the error budget is completely consumed by these inaccuracies and there is no margin left for additional errors due to temperature effects, antenna misalignment, radar vehicle misalignment, or electromagnetic interference effects. Clearly, the radar unit would not meet this accuracy requirement.

Occasional road testing of the radar with an actual calibrated target vehicle is desirable as a check of the overall operation of the radar. Clearly, these tests should be done with a vehicle having a speedometer uncertainty less than 1 mph. These tests will help in assessing the errors that are not evaluated by the calibrator, such as the effects of mechanical misalignment of the radar vehicle and the variety of vehicle signatures.

9. CONCLUSIONS

This paper describes an inexpensive, easy-to-use electronic calibrator that can be used to improve the credibility of across-the-road type radars. It can warn the user of actual failures that may result in erroneous speed readings. Regular documented use of the calibrator can also indicate trends in the operation of the radar that may suggest that a particular unit should be scheduled for maintenance, thus avoiding the unexpected failure of a system and the expensive consequences of that uncertainty.

The test results on a commercial across-the-road system unit show the value of using the calibrator for evaluations. Not only can the radar be tested for correct speed readout, but, often, the sources of the errors can be diagnosed. This allows the testing laboratory to make more informed decisions about the qualifications of a particular radar unit and, therefore, to better predict how the radar will function in actual use. The calibrator is capable of more complex combinations of sideband and chirp that enhance this diagnostic capability, but these are beyond the scope of this report.

The authors wish to express their appreciation to Brian Trayner of the National Health and Transportation Safety Administration for funding this work, and to Dr. George Leiberman for his vital contributions to the effective management of the project.

We are further indebted to our division chief, Dr. Dennis Friday, our group leader, Dr. Motohisa Kanda, and our readers, Manley Weidman, Nicholas Di Minco, Dr. Matt Young, and Dr. Carl Stubenrauch. The accuracy of the material presented in this Tech Note, as well as its readability, have benifited greatly from their suggestions.

11. REFERENCES

[1] Harry, R.; Amos, S.J.; and Pratt A.P.S.; ***An Examination of Doppler Radar Speedometers Incorporating Photography.*** St. Albans, United Kingdom: Police Scientific Development Branch (PSDB), 1991.

[2] Berger, F.B., "The Nature of Doppler Velocity Measurement," IRE Transactions on Aeronautical and Navigational Electronics, September 1957.

[3] Fisher, P.D., "Shortcomings of Radar Speed Measurement," IEEE Spectrum, December 1980, pp. 28-31.

[4] Mennie, D., "Helping Speeders Beat the Radar Rap," IEEE Spectrum, August 1978, pp. 38-42.

[5] Rihaczek, A. W., ***Principles of High Resolution Radar.*** Los Altos, CA: Peninsula Publishers, 1985.

[6] ***Radar Equipment for the Measurement of the Speed of Vehicles***, Organisation Internationale de Metrologie Legale (OIML): Paris, 1991.

[7] Edde, B., ***Radar: Principles, Technology, and Applications.*** Englewood Cliffs, NJ: Prentice Hall, 1993.

[8] Skolnik, M.I., ***Introduction to Radar Systems.*** New York, NY: Mc Graw Hill, 1980.

[9] Bodard, P., "They Have Lasers, and We Captured One for a Test," Car and Driver Magazine, April, 1992.

[10] Gabel, R.A., Roberts, R. G., ***Signals and Linear Systems.*** New York, NY: John Wiley and Sons, 1988.

[11] Dwight, H.B., ***Tables of Integrals and Other Mathematical Data.*** New York, NY: Macmillan Publishing Co., 1961.

[12] Gupta, K.C., Garg, R., Chadha, R., ***Computer-Aided Design of Microwave Circuits.*** Norwood, MA: Artech House, 1981.

[13] Engen, G.F., ***Microwave Circuit Theory and Foundations of Microwave Metrology.*** London, UK: Peter Pereginus Ltd., 1992.

[14] Collin, R.E., ***Foundations for Microwave Engineering.*** New York, NY: McGraw Hill, 1966.

[15] Gupta, K.C., Garg, R., ***Microstrip Lines and Slotlines.*** Norwood, MA: Artech House, 1979.

[16] Johnk, C.T.A., ***Engineering Electromagnetic Fields and Waves.*** New York, NY: John Wiley and Sons, 1988.

APPENDIX A

FOURIER ANALYSIS OF THE CALIBRATOR PERFORMANCE

This appendix presents the analysis of the signal that is reflected from the calibrator when switched at a constant rate. The signal is expanded in a complex exponential Fourier series representation [10], and an analytical expression for the Fourier coefficients is developed. The expression facilitates the understanding of the calibrator operation.

The transmitted CW signal from the radar under test can be represented in analytic form [5] as

$$S_i = A e^{j2\pi f_r t} , \qquad \textbf{(A.1)}$$

where A is the complex amplitude and f_r is the radar transmit frequency.

The signal that is reflected back to the radar under test is given by

$$s_r(t) = e^{j2\pi f_r t} [c + a(t)] , \qquad \textbf{(A.2)}$$

where c is the complex amplitude due to scattering from both the calibrator and possibly other nearby objects, and $a(t)$ is the modulated component generated solely by the calibrator. It is the modulated component $a(t)$ which provides a suitable Doppler signature for the verification of radar performance. If the calibrator is operated in the mode for which each of the N phase states has equal duration (no chirping), and the switching sequence is repeated every T_s seconds, the resulting modulated component is given by

$$a(t) = \Gamma(t) e^{j\theta(t)} ,$$

$$\Gamma(t) = A_m, \ (m-1)\frac{T_s}{N} < t \le m\frac{T_s}{N}$$

$$\theta(t) = \theta_m, \ (m-1)\frac{T_s}{N} < t \le m\frac{T_s}{N} \qquad \textbf{(A.3)}$$

$$m = 1, 2, \ldots, N ,$$

where A_m and θ_m are amplitude and phase values that are constant for each value of m. In order to achieve optimal calibrator performance, amplitude and phase shifts to be realized are given by

$$A_m = b, \quad \theta_m = \frac{\pm 2\pi m}{N}, \qquad m = 1,2, \ldots, N, \tag{A.4}$$

where b is a constant. A positive sign in eq (A.4) denotes an increasing phase sequence (this simulates an approaching vehicle and a minus sign denotes a decreasing phase sequence (for a receding vehicle). The calibrator functions most effectively when the amplitudes of each of the switch states are exactly equal and the phase shifts increase or decrease in fractional increments of 2π rad over the total number of phase shift states, N. In the case of the NIST unit N=5, so eq (A.4) yields an optimal increment of $2\pi/5$ rad or 72°.

In order to understand precisely how the calibrator functions, the modulated term can be expanded in a complex exponential Fourier series as [10]

$$a(t) = \sum_{n=-\infty}^{\infty} d_n e^{\frac{j2\pi nt}{T_s}}, \tag{A.5}$$

with

$$d_m = \frac{1}{T_s} \int_0^{T_s} a(t)\, e^{\frac{-j2\pi mt}{NT_s}}\, dt. \tag{A.6}$$

From eqs (A.5) and (A.1), the modulated signal is periodic with period T_s with sidebands that are located on both sides of the carrier frequency f_r, at intervals corresponding to integer harmonics of the fundamental switching frequency $1/T_s$. The complex amplitudes of these sidebands are given by [10] Applying eqs. (A.3) and (A.5) to (A.6) yields

-

$$d_m = \frac{1}{T_s} \sum_{p=0}^{N-1} \int_0^{T_s/N} e^{\frac{j2\pi p}{N}} e^{-j\frac{2\pi m}{T_s}(t+pT_s/N)}\, dt. \tag{A.7}$$

Applying a suitable change of variable to the integral in eq (A.7) obtains the simplified result

$$d_m = \frac{1}{T_s} \sum_{p=0}^{N-1} e^{\frac{j2p\pi}{N}(m-1)} \int_0^{Ts/N} e^{\frac{-j2\pi mx}{T_s}}\, dx. \tag{A.8}$$

Equation (A.8) is a product of a geometric series and a simple integral with an exponential integrand, both of which can be readily evaluated. Using results tabulated in Dwight [11] yields after some simplification

$$d_m = \left(\frac{-1}{j2\pi m}\right) e^{\frac{j\pi}{N}(N-1)(m-1)} \left(e^{\frac{-j2\pi m}{N}} - 1\right) \frac{\sin[\pi(m-1)]}{\sin[\frac{\pi}{N}(m-1)]}$$

$$m = 0, \pm 1, \pm 2, \pm 3, \ldots \quad . \tag{A.9}$$

Equation (A.9) is the final desired result for the complex sideband spectrum assuming a constant amplitude taper and a stepwise increasing phase taper.

Equation (A.9) indicates that the three nonzero harmonics, closest to the carrier frequency of the radar under test occur at frequencies of f_r+1/T_s, $f_r+(N+1)/T_s$, $f_r-(N-1)/T_s$, and the locations of these frequencies are depicted in Figure 15. The dominant reflected signal component occurs at the first of these frequencies, and it is shifted above the radar carrier by the fundamental switching frequency $1/T_s$. The two other harmonic components are removed from the radar carrier frequency by $(N-1)$ and

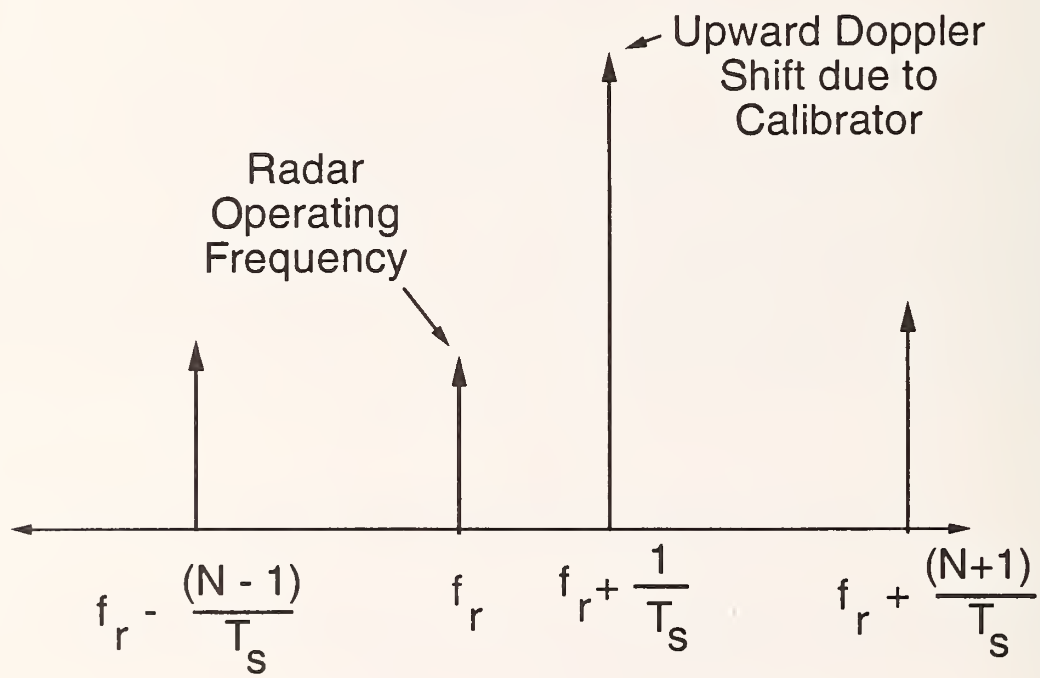

Figure 15. Reflected signal spectrum with an increasing phase sequence.

$(N+1)$ times the fundamental switching frequency.

The fact that all of the other sidebands between the fundamental and the $(N-1)$th harmonic have zero amplitude is absolutely vital to the success of the switched reflector concept. For a suitable choice of N, the radar under test filters out all of the sidebands except for the fundamental at $1/T_s$ which effectively makes the switched reflector a single sideband modulator that shifts the frequency of the radar under test up by an amount $1/T_s$, which simulates a vehicle approaching at a constant rate. If the phase progression specified in eq (A.4) is reversed, the sideband positions are transposed with respect to the radar carrier frequency, and the calibrator shifts the reflected frequency down by $1/T_s$ which simulates a receding vehicle.

In the case of the NIST calibrator with $N=5$, the next higher harmonic of the fundamental switching frequency is the fourth. If the fundamental switching frequency is set to correspond to a Doppler shift of 55 mph for the radar under test, the next reflected component occurs at a Doppler shift corresponding to 220 mph, which will not be processed by commercial radar units. The selection of $N=5$ in the NIST calibrator is therefore sufficient for the unit to function as a "virtual" single sideband modulator for the evaluation of commercially available across-the-road radar systems

APPENDIX B

REFLECTIVE PHASE SHIFTER DESIGN CONSIDERATIONS

This appendix explains the design issues that are involved in obtaining a proper reflective phase shifter performance. The design equations are first introduced and discussed, and then general design procedures and guidelines are given.

For a single-pole, N-position switch, the microwave performance at each switch position can be represented in terms of two-port scattering parameters. Scattering parameters are highly useful since they can readily be measured using vector network analyzers. The measured data obtained is then incorporated into a linear microwave network simulator for the purpose of assessing and optimizing the calibrator performance [12].

$$b_1^m = S_{11}^m a_1^m + S_{12}^m a_2^m$$

$$b_2^m = S_{21}^m a_1^m + S_{22}^m a_2^m \, , \tag{B.1}$$

The switch in Figure 16 can be characterized in terms of its scattering parameters as

where $m=1,2,\ldots,N$ denotes the switch position, S denotes the network scattering parameters, and the a,b terms are the incident and reflected wave variables at the switch ports. The coefficients S_{11} and S_{22} are the switch reflection coefficients obtained with a matched (50 Ω) resistive load; S_{12} and S_{21} are the corresponding switch transmission coefficients, also obtained for a matched load [13]. Since PIN

diode microwave switches are linear and passive, reciprocity [14] demands that $S_{12}=S_{21}$. If the S-parameters for the switch are known, the performance at port 1 can be determined for an arbitrary load termination on port two. Assuming that the termination on port 2 has a complex reflection denoted by Γ_L, the wave variables at port 2 of the switch are interrelated by

$$a_2^m = \Gamma_L^m b_2^m \, . \tag{B.2}$$

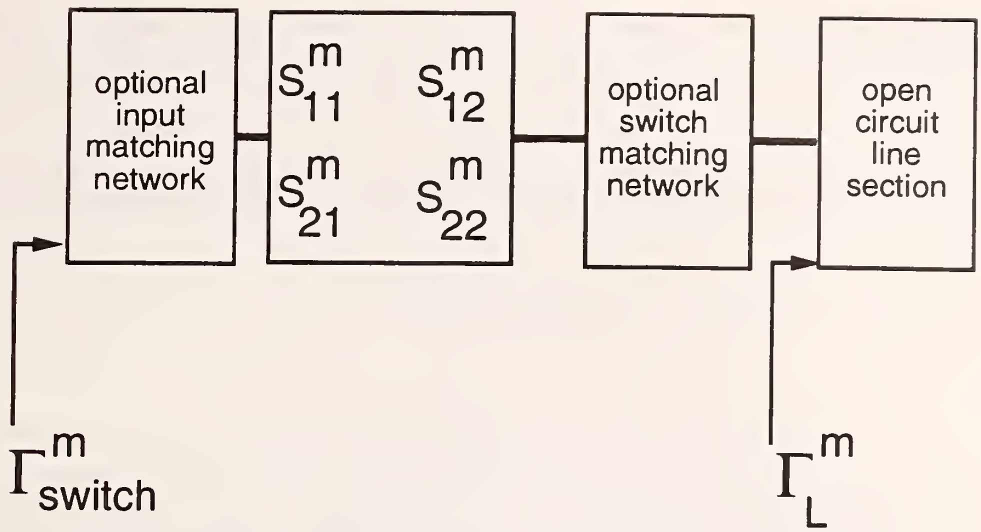

Figure 16. Microwave network representation of the switch section.

If eq (B.1) is applied to eq (B.2) and the ratio is taken of the reflected to incident wave variables at port 1, we obtain the input reflection coefficient of the switch

$$\frac{b_1^m}{a_1^m} = \Gamma_{switch}^m = S_{11}^m + \frac{S_{12}^m S_{21}^m \Gamma_L^m}{1 - S_{22}^m \Gamma_L^m} . \tag{B.3}$$

The input reflection coefficient is a complicated function of the switch scattering parameters and the load reflection coefficient. The input reflection coefficient to the switch determines the magnitude and phase of the signal that is reflected back to the radar under test.

The functional dependence given in eq (B.3) can be simplified significantly through proper microwave design. If the magnitudes of switch parameters S_{11} and S_{22} are small, or can be reduced by the use of matching networks (see Figure 16); the switch reflection coefficient simplifies to

$$\Gamma_{switch}^m = (S_{12}^m)^2 \; \Gamma_L^m . \tag{B.4}$$

For a switch that has a good input and output match, the input reflection coefficient is a simple product of the two-way switch transmission characteristics and the load reflection coefficient.

One viable approach to achieving a desired switch reflection phase at a given switch position is to place a length of open-circuit transmission line at the switch output. The desired phase can be synthesized by simply adjusting the length of the line. If the switch is well matched, reflection phases over the entire range of 0° to 360° can be realized. Thus combining open-circuit transmission lines and input/output matching networks permit the synthesis of arbitrary phase sequences. Assuming that the magnitudes of switch transmission parameters do not vary much from one switch position to the next (this should be the case for any suitably designed switch), the desired switched reflector performance can readily be achieved.

The reflection coefficient at the input of an open-circuit section of coaxial transmission line of length h^m is given by

$$\Gamma_L = e^{-j\theta_{line}} ,$$

$$\theta_{line} = 2\, k_{eff}\, h^m , \tag{B.5}$$

where k_{eff} is the effective wavenumber of the transmission line section. In terms of the material properties of the dielectric insulator of the coaxial line, the effective wavenumber is given by

$$k_{eff} = 2\pi f_r \sqrt{\mu_0 \varepsilon_0 \varepsilon_r} , \tag{B.6}$$

where $\mu_0 = 4\pi \times 10^{-7}$, $\varepsilon_0 = 8.85 \times 10^{-12}$, and ε_r is the relative dielectric of the insulating medium, which must be determined either by measurement or manufacturer-supplied data. Equation (B.5) is also valid for printed-circuit microstrip transmission structures, but a formula given in [12] that accounts for dispersion effects must be used in place of eq (B.6) to obtain sufficient accuracy.

Equation (B.5) assumes a perfect open circuit, and fringing effects are ignored. Open-circuit coax and microstrip lines have a fringing capacitance associated with them [15] that effectively lengthens the line, so if the line section lengths are computed from eq (B.6), the lengths will have to be made somewhat shorter to obtain the correct phases. Making open-circuit microstrip and coaxial line sections shorter is straightforward and simple, and requires minimal time. The accurate computation of fringing effects is involved and is beyond the scope of this work. In the case of microstrip lines, empirical formulas can be found in [15]. Microstrip fringing effects derived from theory or measurement data are often incorporated into commercially available microwave network simulators. If we use coaxial cable sections, the input reflection phase that includes fringing effects can be directly measured with a vector network analyzer without having to compute an additional correction.

Now the total reflection phase shift provided by the combination of the open-circuit line and the switch is given by

$$\theta = \theta_{line} + \theta_{switch} , \tag{B.7}$$

where θ_{line} is the phase contribution given by eq (B.5), and θ_{switch} is the phase shift provided by the measured transmission characteristics of the switch/matching networks combination. Equation (B.7) indicates that once the switch transmission phase is known, the desired phase shift can be achieved by simply superimposing the transmission phase contribution of an open circuit line section to that of the switch.

The results of the discussion up to this point, along with the experience gained from the construction of the NIST calibrator can be used to generate a systematic design procedure for the reflective phase shifter portion of the radar calibrator. This procedure is summarized in the following steps:

1. Measure the two port S-parameters (magnitude and phase) of the switch at the radar frequency of interest at all of the switch positions using a vector network analyzer or some other suitable measurement system.

2. If the switch reflection coefficient magnitudes $|S_{11}|$ or $|S_{22}|$ are too large, the magnitude of the offending parameter must be reduced using a matching network at the switch input (if $|S_{11}|$ is too large) or at the switch outputs if $|S_{22}|$ is too large. There is no hard and fast rule for the determination of unacceptable values of reflection coefficient magnitudes. Unacceptable levels can only be determined by carrying out an analysis of the switch input reflection characteristics using eq (B.4) for a prescribed set of phase shifts at each of the switch positions. There are a lot of possibilities for matching network designs, and once again there is no hard and fast rule for the type of matching network that must be used. In our calibrator, $|S_{11}|$ was too large so the simple open-circuit shunt stub arrangement of Figure 9 was used on the switch input. This type of matching network can be designed either by incorporating the measured switch S-parameter data into a computerized microwave network simulator, or by using simple Smith chart design procedures that are extensively treated in Johnk [16].

3. After the switch has been matched, the lengths of the open-circuit line sections must be determined. The first step of this procedure is to prescribe the required set of input reflection switch phase shifts that will be realized at the N switch positions. Then the required line input phases must be found from eq (B.7). The line phase shift requirements are then converted into realizable physical lengths using eq (B.6), or, in a more direct fashion, by placing the open-circuit line sections on a vector network analyzer and adjusting the line length until the required phase shift is obtained. The direct method of obtaining required line phase shifts using a network analyzer was used with excellent results in the construction of the NIST calibrator.

4. Once the open-circuit lines are installed on the switch outputs, the design and construction of the calibrator is completed. At this point, the calibrator switch section performance must be verified by measuring the calibrator input reflection phase characteristics at each of the N switch positions. The relative phases from one switch position to the next should be consistent with eq (A.4) of Appendix A for optimal performance. If the results obtained in this step are satisfactory, the design of the microwave portion of the calibrator is complete.

*U.S. GOVERNMENT PRINTING OFFICE 1998-0-673-018/40096

NIST *Technical Publications*

Periodical

Journal of Research of the National Institute of Standards and Technology—Reports NIST research and development in those disciplines of the physical and engineering sciences in which the Institute is active. These include physics, chemistry, engineering, mathematics, and computer sciences. Papers cover a broad range of subjects, with major emphasis on measurement methodology and the basic technology underlying standardization. Also included from time to time are survey articles on topics closely related to the Institute's technical and scientific programs. Issued six times a year.

Nonperiodicals

Monographs—Major contributions to the technical literature on various subjects related to the Institute's scientific and technical activities.

Handbooks—Recommended codes of engineering and industrial practice (including safety codes) developed in cooperation with interested industries, professional organizations, and regulatory bodies.

Special Publications—Include proceedings of conferences sponsored by NIST, NIST annual reports, and other special publications appropriate to this grouping such as wall charts, pocket cards, and bibliographies.

Applied Mathematics Series—Mathematical tables, manuals, and studies of special interest to physicists, engineers, chemists, biologists, mathematicians, computer programmers, and others engaged in scientific and technical work.

National Standard Reference Data Series—Provides quantitative data on the physical and chemical properties of materials, compiled from the world's literature and critically evaluated. Developed under a worldwide program coordinated by NIST under the authority of the National Standard Data Act (Public Law 90-396). NOTE: The Journal of Physical and Chemical Reference Data (JPCRD) is published bi-monthly for NIST by the American Chemical Society (ACS) and the American Institute of Physics (AIP). Subscriptions, reprints, and supplements are available from ACS, 1155 Sixteenth St., NW, Washington, DC 20056.

Building Science Series—Disseminates technical information developed at the Institute on building materials, components, systems, and whole structures. The series presents research results, test methods, and performance criteria related to the structural and environmental functions and the durability and safety characteristics of building elements and systems.

Technical Notes—Studies or reports which are complete in themselves but restrictive in their treatment of a subject. Analogous to monographs but not so comprehensive in scope or definitive in treatment of the subject area. Often serve as a vehicle for final reports of work performed at NIST under the sponsorship of other government agencies.

Voluntary Product Standards—Developed under procedures published by the Department of Commerce in Part 10, Title 15, of the Code of Federal Regulations. The standards establish nationally recognized requirements for products, and provide all concerned interests with a basis for common understanding of the characteristics of the products. NIST administers this program in support of the efforts of private-sector standardizing organizations.

Consumer Information Series—Practical information, based on NIST research and experience, covering areas of interest to the consumer. Easily understandable language and illustrations provide useful background knowledge for shopping in today's technological marketplace.

Order the **above** *NIST publications from: Superintendent of Documents, Government Printing Office, Washington, DC 20402.*

Order the **following** *NIST publications—FIPS and NISTIRs—from the National Technical Information Service, Springfield, VA 22161.*

Federal Information Processing Standards Publications (FIPS PUB)—Publications in this series collectively constitute the Federal Information Processing Standards Register. The Register serves as the official source of information in the Federal Government regarding standards issued by NIST pursuant to the Federal Property and Administrative Services Act of 1949 as amended, Public Law 89-306 (79 Stat. 1127), and as implemented by Executive Order 11717 (38 FR 12315, dated May 11, 1973) and Part 6 of Title 15 CFR (Code of Federal Regulations).

NIST Interagency Reports (NISTIR)—A special series of interim or final reports on work performed by NIST for outside sponsors (both government and non-government). In general, initial distribution is handled by the sponsor; public distribution is by the National Technical Information Service, Springfield, VA 22161, in paper copy or microfiche form.

U.S. Department of Commerce
National Institute of Standards and Technology
325 Broadway
Boulder, Colorado 80303-3328